J. Fluid Mech. (2012), *vol.* 700, *pp.* 63–76.
doi:10.1017/jfm.2012.91

Release of a viscous power-law fluid over an inviscid ocean

Samuel S. Pegler†, John R. Lister and M. Grae Worster

Institute of Theoretical Geophysics, Department of Applied Mathematics and Theoretical Physics, CMS, Wilberforce Road, Cambridge CB3 0WA, UK

(Received 17 May 2011; revised 10 February 2012; accepted 12 February 2012; first published online 17 April 2012)

We consider the two- and three-dimensional spreading of a finite volume of viscous power-law fluid released over a denser inviscid fluid and subject to gravitational and capillary forces. In the case of gravity-driven spreading, with a power-law fluid having strain rate proportional to stress to the power n, there are similarity solutions with the extent of the current being proportional to $t^{1/n}$ in the two-dimensional case and $t^{1/2n}$ in the three-dimensional case. Perturbations from these asymptotic states are shown to retain their initial shape but to decay relatively as t^{-1} in the two-dimensional case and $t^{-3/(n+3)}$ in the three-dimensional case. The former is independent of n, whereas the latter gives a slower rate of relative decay for fluids that are more shear-thinning. In cases where the layer is subject to a constraining surface tension, we determine the evolution of the layer towards a static state of uniform thickness in which the gravitational and capillary forces balance. The asymptotic form of this convergence is shown to depend strongly on n, with rapid finite-time algebraic decay in shear-thickening cases, large-time exponential decay in the Newtonian case and slow large-time algebraic decay in shear-thinning cases.

Key words: gravity currents, non-Newtonian flows, thin films

1. Introduction

In a recent paper, Pegler & Worster (2012) consider the gravitational spreading of a layer of viscous Newtonian fluid supplied at constant flux, flowing over a denser inviscid fluid. Such a layer receives negligible traction from both the inviscid fluid below it and the air above it, which implies that its horizontal velocity undergoes very little vertical shear and its dynamics are dominated by extensional viscous stresses. In this paper, we investigate the example of a fixed volume of viscous power-law fluid that spreads under the influence of gravitational and capillary forces. Our primary motivation is to understand the stability of such flows to perturbation and to determine the evolution of the layer towards self-similar propagation. Our interest in power-law rheologies stems from the context of ice-shelf dynamics, where the flow is commonly modelled using a power-law shear-thinning constitutive relation known as Glen's flow law (Paterson 1994).

The problem of a viscous Newtonian fluid of constant volume spreading at the interface between inviscid fluids has been considered previously in two dimensions by

† Email address for correspondence: ssp23@cam.ac.uk

DiPietro & Cox (1979) and in three dimensions by Koch & Koch (1995), both in the case of negligible surface tension. DiPietro & Cox (1979) and Koch & Koch (1995) calculate similarity solutions that describe the large-time asymptotic evolution of two-dimensional and axisymmetric finite-volume releases, respectively. Both of these similarity solutions exhibit a uniform thickness profile with no horizontal pressure gradients in the interior. It is thus notable that the spread of the entire layer in these asymptotic states is driven solely by the hydrostatic pressure discontinuity at their edges; they provide excellent demonstrations of the long-range transmission of forces that can occur through floating viscous layers of this kind.

Koch & Koch (1995) demonstrate numerically that a spherical blob of viscous fluid released beneath the surface of a denser fluid of much lower viscosity converges towards the axisymmetric similarity solution. These findings are supported by laboratory experiments by Dorsey & Manga (1998), which show convergence of the experimental spreading rate towards that of the similarity solution. In this paper, we extend these studies to allow for both a power-law rheology and a constraining surface tension and to calculate solutions for the evolution of the layer towards self-similar propagation.

In the case of a two-dimensional finite-volume release subject to negligible surface tension, we can integrate the model equations analytically to determine the evolution of finite-amplitude perturbations. The equations describing an axisymmetric finite-volume release are complicated fundamentally by contributions due to hoop stresses (Pegler & Worster 2012). In this case, we perform a linear perturbation analysis to calculate analytically the evolution of small axisymmetric perturbations from the uniform asymptotic state. A significant contrast can be drawn between the behaviour of the finite-volume release studied here and that of the constant-flux delivery studied by Pegler & Worster (2012). In the latter case, the presence of the source precludes a global evolution of the thickness towards a state of uniform thickness, and the large-time flow is consequently shown to exhibit much greater structure.

The role of surface tension was found to be an important consideration in the experimental study of Pegler & Worster (2012). In order to understand some aspects of its influence, we determine here the evolution of an axisymmetric finite-volume release subject to a constraining surface tension. We model the influence of surface tension to leading order by assuming that it acts only at the front of the layer to give a stress of magnitude that is inversely proportional to the thickness near the front. This model has been developed previously in the context of float-glass manufacture (Howell 1994).

The case of a spreading surface tension, which we do not consider here, has been studied in the context of very viscous oil slicks by DiPietro & Cox (1979). They developed a higher-order surface-tension model to account for the development of a thin precursor film ahead of the bulk of the layer. Their analysis suggests that the dynamics in this case may transition to the gravity-driven regime described in the preceding paragraphs. Other studies of oil-slick mechanics, such as those of Hoult (1972) and Foda & Cox (1980), consider regimes in which the layer is driven by a spreading surface tension and retarded by the underlying viscous drag of the ocean, rather than the extensional viscous stresses in the slick.

We begin in § 2 by reviewing briefly our model for a viscous layer of fluid flowing over a denser inviscid fluid. In § 3, we consider the evolution of perturbations from the two- and three-dimensional similarity solutions. In § 4, we calculate solutions to generalized model equations that include the effects of surface tension.

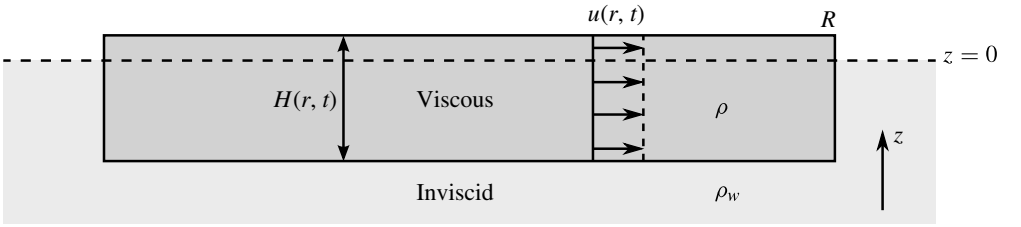

FIGURE 1. Schematic cross-section of the uniform similarity solution (3.19) that describes the large-time three-dimensional finite-volume release.

2. Model equations

Consider a thin layer of power-law viscous fluid of density ρ flowing on top of an inviscid stationary ocean of greater density ρ_w, as shown schematically in the case of uniform thickness in figure 1. The horizontal velocity $\boldsymbol{u}(\boldsymbol{x}, t)$ of such a layer is governed to leading order by the force-balance equation

$$\boldsymbol{\nabla}(\mu H \boldsymbol{\nabla}\cdot\boldsymbol{u}) + \boldsymbol{\nabla}\cdot(\mu H \boldsymbol{e}) = \tfrac{1}{2}\rho g' H \boldsymbol{\nabla} H, \tag{2.1}$$

where $H(\boldsymbol{x}, t)$ is the thickness, $\boldsymbol{e} \equiv (1/2)[\boldsymbol{\nabla}\boldsymbol{u} + (\boldsymbol{\nabla}\boldsymbol{u})^{\mathrm{T}}]$ is the horizontal rate-of-strain tensor, $g' \equiv (\rho_w - \rho)g/\rho_w$ is the reduced gravity, g is the acceleration due to gravity and $\boldsymbol{\nabla}$ is the horizontal part of the gradient operator. Equation (2.1) follows from a generalization of the derivation of the Newtonian case (DiPietro & Cox 1979; Pegler & Worster 2012). We impose the power-law viscosity

$$\mu = \tilde{\mu}\left[\tfrac{1}{2}\boldsymbol{E}:\boldsymbol{E}\right]^{m/2} \equiv \tilde{\mu}\left[\tfrac{1}{2}\{\boldsymbol{e}:\boldsymbol{e} + (\boldsymbol{\nabla}\cdot\boldsymbol{u})^2\}\right]^{m/2}, \tag{2.2}$$

where $\boldsymbol{E}$ is the full three-dimensional rate-of-strain tensor, and $\tilde{\mu}$ and m are constants. The constant m is related to the power-law exponent n by $m \equiv 1/n - 1$. The Newtonian case is given by $n = 1$ $(m = 0)$; shear-thinning and shear-thickening cases are given by $n > 1 (m < 0)$ and $n < 1$ $(m > 0)$, respectively. In the context of glacial ice shelves, a power-law exponent of $n = 3$ is commonly used in Glen's flow law, corresponding to shear-thinning (Paterson 1994). Having determined $\boldsymbol{u}$ by solving (2.1)–(2.2) subject to suitable boundary conditions on $\boldsymbol{u}$, the evolution of the thickness H is described by the continuity equation

$$\frac{\partial H}{\partial t} + \boldsymbol{\nabla}\cdot(H\boldsymbol{u}) = 0. \tag{2.3}$$

In this paper, we apply a dynamic boundary condition at edges of the layer that represents a balance between the depth-integrated stress in the layer and the combined effect of the hydrostatic pressure of the ocean exerted horizontally upon it and any capillary forces. Note that, although capillary forces are negligible over the small curvatures of the interior of the layer, capillary forces can be large at the edges where the assumed thinness of the layer implies significant curvature of its surface. By performing a horizontal force balance on a region that extends from a point $\boldsymbol{x} = \boldsymbol{X}$ on the edge to a nearby interior point where the curvature is small, Howell (1994) determined the leading-order dynamic boundary condition

$$2\mu[(\boldsymbol{\nabla}\cdot\boldsymbol{u})\boldsymbol{n} + \boldsymbol{e}\cdot\boldsymbol{n}] = \left(\tfrac{1}{2}\rho g' H - \gamma H^{-1}\right)\boldsymbol{n} \qquad (\boldsymbol{x} = \boldsymbol{X}), \tag{2.4}$$

where $\boldsymbol{n}$ is the unit horizontal normal to the edge. The constant $\gamma \equiv \gamma_{va} + \gamma_{vw} - \gamma_{aw}$ is a coefficient of total surface tension composed of the interfacial surface tensions between the layer and the air γ_{va}, the layer and the ocean γ_{vw}, and the ocean and the air γ_{aw}.

We expect (2.4) to be appropriate only if the surface tension is zero or constraining, so $\gamma \geqslant 0$. If $\gamma < 0$, experiments with oil on water (Foda & Cox 1980) show that a molecularly thin layer of oil propagates rapidly in front of the bulk of the oil. Clearly, the presence of this thin layer of fluid in front of the bulk changes the interfacial forces so that (2.4) does not apply.

3. Finite-volume release subject to negligible surface tension

We begin by considering the case of negligible surface tension $\gamma = 0$ in which the motion of the layer is driven solely by horizontal buoyancy gradients.

3.1. *Two-dimensional release*

Consider a two-dimensional viscous layer of thickness $H(x, t)$ and velocity $u(x, t)\hat{\boldsymbol{x}}$. The evolution of the layer is governed by (2.1) and (2.3), which take the two-dimensional forms

$$2\frac{\partial}{\partial x}\left(\mu H \frac{\partial u}{\partial x}\right) = \frac{1}{2}\rho g' H \frac{\partial H}{\partial x}, \tag{3.1}$$

$$\frac{\mathrm{D}H}{\mathrm{D}t} = -H\frac{\partial u}{\partial x}, \tag{3.2}$$

respectively, where $\mathrm{D}/\mathrm{D}t \equiv \partial/\partial t + u\,\partial/\partial x$ is the material derivative. The effective viscosity (2.2) takes the two-dimensional form

$$\mu = \tilde{\mu}\left|\frac{\partial u}{\partial x}\right|^m. \tag{3.3}$$

Let us assume that the layer has an edge at $x = X(t)$. A boundary condition for solution of (3.1) is given by the dynamic condition (2.4), which takes the two-dimensional form

$$2\mu\frac{\partial u}{\partial x} = \frac{1}{4}\rho g' H \quad (x = X). \tag{3.4}$$

Equations (3.1) and (3.4) are invariant under Galilean transformation and therefore solution of (3.1) for u requires a further condition to fix the velocity at a point; otherwise, the layer is free to drift sideways. However, for the purposes of discussing the convergence towards self-similarity, we require only $\partial u/\partial x$ and hence we impose no further conditions on the velocity field. We assume the initial thickness profile

$$H = H_0(x) \quad (t = 0). \tag{3.5}$$

Equation (3.1) can be integrated subject to condition (3.4) to give

$$2\mu\frac{\partial u}{\partial x} = \frac{1}{4}\rho g' H \tag{3.6}$$

at all points of the layer. Equation (3.6) shows that the buoyancy-induced extension of the layer is proportional to the thickness H at each point. Note that, although this equation relates local variables, its right-hand side represents a non-local integration of the horizontal buoyancy gradients from the front X to the point x. Equation (3.6)

implies that the rate of extension is always positive, so we can remove the modulus from the right-hand side of (3.3). Using (3.3) to eliminate μ from (3.6), we determine that

$$\frac{\partial u}{\partial x} = \left(\frac{g'H}{8\tilde{\nu}}\right)^n, \tag{3.7}$$

where $\tilde{\nu} \equiv \tilde{\mu}/\rho$ is a constant and $n \equiv 1/(1+m)$. Using (3.7) to substitute for $\partial u/\partial x$ in (3.2), we deduce that

$$\frac{\mathrm{D}H}{\mathrm{D}t} = -H\left(\frac{g'H}{8\tilde{\nu}}\right)^n, \tag{3.8}$$

which describes the material evolution of the thickness and shows, in particular, that thicker parts of the layer are thinned more rapidly. Buoyancy forces therefore act to dissipate any non-uniformities in the thickness profile. This can be contrasted with the evolution of a shear-dominated viscous gravity current at a fluid interface, in which the rate of thinning also depends on the slope of the current $\partial H/\partial x$ (Lister & Kerr 1989) and the corresponding asymptotic similarity solution has non-uniform thickness.

Let $H_L(x_0, t)$ denote the thickness at time t of the material fluid element that had location $x = x_0$ at $t = 0$. We can integrate (3.8) subject to (3.5) to obtain the solution for the material evolution of the thickness,

$$\frac{1}{H_L^n} = \frac{1}{H_0^n} + n\left(\frac{g'}{8\tilde{\nu}}\right)^n t, \tag{3.9}$$

(cf. Robison, Huppert & Worster 2010). By taking the reciprocal of both sides of (3.9) and expanding in powers of t^{-1}, we determine that

$$H_L \sim \frac{8\tilde{\nu}}{g'\,(nt)^{1/n}}\left[1 - \frac{1}{n^2}\left(\frac{8\tilde{\nu}}{g'H_0}\right)^n t^{-1}\right], \tag{3.10}$$

for large times. This equation shows that the thickness of the layer converges towards a uniform similarity solution $8\tilde{\nu}/g'\,(nt)^{1/n}$ with a non-uniform first-order correction that decays as t^{-1} at large times relative to the similarity solution. This rate of relative decay is algebraic, which is a generic feature of perturbations to similarity solutions that evolve algebraically in time (cf. Leppinen & Lister 2003). The time scale $n^{-2}\,(8\tilde{\nu}/g'H_0)^n$ characterizes the time beyond which buoyancy forces have had significant influence on the flow (cf. Pegler & Worster 2012). The Newtonian case $n = 1$ of the leading-order similarity solution in (3.10) has been calculated by DiPietro & Cox (1979).

3.2. *Three-dimensional release*

Consider an isolated axisymmetric layer of volume V with thickness $H(r, t)$. Left alone, the layer will be driven to spread radially under the influence of buoyancy forces. The velocity of the layer $u(r, t)$ is described by the axisymmetric form of (2.1),

$$\frac{\partial}{\partial r}\left[\mu H(\boldsymbol{\nabla}\cdot\boldsymbol{u} + e_{rr})\right] + \mu\frac{H}{r}(e_{rr} - e_{\theta\theta}) = \frac{1}{2}\rho g'H\frac{\partial H}{\partial r}, \tag{3.11}$$

where $e_{rr} = \partial u/\partial r$ and $e_{\theta\theta} = u/r$ are the rates of radial and azimuthal extension, and the viscosity (2.2) is given by

$$\mu = \tilde{\mu}\left[\tfrac{1}{2}\{e_{rr}^2 + e_{\theta\theta}^2 + (\boldsymbol{\nabla}\cdot\boldsymbol{u})^2\}\right]^{m/2}. \tag{3.12}$$

The last term on the left-hand side of (3.11) represents the viscous stress due to azimuthal extension, or hoop stress. Its presence precludes the first integral of the force-balance equation (3.11) that was possible with the two-dimensional analogue (3.1). In the axisymmetric case, there is no analogue of (3.6) because the rate of extension at any point of the layer is influenced non-locally by the hoop stresses throughout the layer. Nevertheless, (3.11) shows that the qualitative effect of the buoyancy force is to extend the layer radially.

The evolution of H is described by (2.3), which takes the axisymmetric form

$$\frac{\partial H}{\partial t} + \frac{1}{r}\frac{\partial}{\partial r}(rHu) = 0. \tag{3.13}$$

We impose a regularity condition at the origin, namely

$$u = 0 \quad (r = 0), \tag{3.14}$$

which provides one condition for solution of (3.11). A second is given by the dynamic condition (2.4) which, in the absence of surface tension, takes the axisymmetric form

$$\mu\left[2\frac{\partial u}{\partial r} + \frac{u}{r}\right] = \frac{1}{4}\rho g' H \quad (r = R), \tag{3.15}$$

where $R(t)$ denotes the radial position of the edge, or *front*, of the layer. Conservation of mass at the front implies that its position evolves according to

$$\dot{R} = u(R, t), \tag{3.16}$$

where we use a dot to denote $\mathrm{d}/\mathrm{d}t$. Equations (3.13), (3.14) and (3.16) ensure that no mass enters the system and are consistent with a constant total volume

$$\int_0^R 2\pi r H \,\mathrm{d}r = V. \tag{3.17}$$

We assume an initial condition

$$R(0) = 0, \tag{3.18}$$

corresponding to a point release.

There are only two independent dimensional parameters in the system above, namely $\tilde{\mu}/\rho g'$ and V. To form a horizontal length scale from these parameters, it is necessary to incorporate an explicit dependence on time t. The system therefore supports similarity solutions, which can be determined as

$$H_0 = \frac{12\tilde{\nu}_m}{g'}(2nt)^{-1/n}, \quad u_0 = \frac{r}{2nt}, \quad R_0 = \left(\frac{Vg'}{12\pi\tilde{\nu}_m}\right)^{1/2}(2nt)^{1/2n}, \tag{3.19}$$

where $\tilde{\nu}_m \equiv \tilde{\mu}_m/\rho \equiv 3^{m/2}\tilde{\mu}/\rho$. This uniformly straining similarity solution is the axisymmetric analogue of the two-dimensional asymptotic state described by the leading-order term in (3.10). The Newtonian case of (3.19) with $n = 1$ has been determined by Koch & Koch (1995).

To understand the evolution of the layer from general axisymmetric initial conditions towards the similarity solution (3.19), we consider the evolution of a small perturbation from the asymptotic state (3.19) made at time $t = t_0$, namely

$$H(r, t_0) = H_0(t_0) + \epsilon H_1(r, t_0), \quad R(t_0) = R_0(t_0) + \epsilon R_1(t_0), \tag{3.20}$$

where $\epsilon \ll 1$, and H_0, H_1, R_0 and R_1 are of equal order. We assume that the perturbation (3.20) leaves the volume of the layer unchanged so (3.17) is unaffected.

Let us define the scales

$$\mathscr{M} \equiv \tilde{\mu}_m t_0^{-m}, \quad \mathscr{H} \equiv \frac{\mathscr{M}}{\rho g' t_0}, \quad \mathscr{L} \equiv \left(\frac{V}{2\pi\mathscr{H}}\right)^{1/2}, \tag{3.21}$$

which characterize the viscosity, thickness and radius of the similarity solution (3.19) at the time t_0 at which the perturbation (3.20) is made. We use (3.21) to non-dimensionalize the system (3.11)–(3.18) according to

$$x \equiv \mathscr{L}\hat{x}, \quad t \equiv t_0\hat{t}, \quad H \equiv \mathscr{H}\hat{H}, \quad u \equiv (\mathscr{L}/t_0)\hat{u}, \quad \mu \equiv \mathscr{M}\hat{\mu}. \tag{3.22}$$

On dropping the hat diacritic, (3.11) and (3.13) become

$$\frac{\partial}{\partial r}\left[\mu H\left(2\frac{\partial u}{\partial r} + \frac{u}{r}\right)\right] + \mu H\frac{\partial}{\partial r}\left(\frac{u}{r}\right) = \frac{1}{2}H\frac{\partial H}{\partial r}, \tag{3.23}$$

$$\frac{\partial H}{\partial t} + \frac{1}{r}\frac{\partial}{\partial r}(rHu) = 0, \tag{3.24}$$

and the viscosity (3.12) becomes

$$\mu = \left[\frac{1}{6}\left\{\left(\frac{\partial u}{\partial r}\right)^2 + \left(\frac{u}{r}\right)^2 + \left(\frac{1}{r}\frac{\partial}{\partial r}(ru)\right)^2\right\}\right]^{m/2}. \tag{3.25}$$

Boundary conditions (3.14) and (3.15) become

$$u = 0 \qquad (r = 0), \tag{3.26}$$

$$\mu\left[2\frac{\partial u}{\partial r} + \frac{u}{r}\right] = \frac{1}{4}H \quad (r = R), \tag{3.27}$$

and the frontal-evolution and volume-conservation equations (3.16) and (3.17) become

$$\dot{R} = u(R, t), \quad \int_0^R rH\,\mathrm{d}r = 1, \tag{3.28a,b}$$

respectively. The non-dimensional form of the similarity solution (3.19), which is a solution of (3.23)–(3.28), can be written

$$H_0 = 12E^{1/n}, \quad u_0 = Er, \quad R_0 = 6^{-1/2}E^{-1/2n}, \quad \mu_0 = E^m, \tag{3.29}$$

where $E(t) \equiv 1/2nt$ is the (uniform) rate of extension.

To determine the evolution of the perturbation, we substitute expansions of the form

$$H(r, t) = H_0(t) + \epsilon H_1(r, t) + \cdots, \tag{3.30}$$

$$u(r, t) = u_0(r, t) + \epsilon u_1(r, t) + \cdots, \tag{3.31}$$

$$R(t) = R_0(t) + \epsilon R_1(t) + \cdots, \tag{3.32}$$

$$\mu(r, t) = \mu_0(t) + \epsilon\mu_1(r, t) + \cdots, \tag{3.33}$$

into (3.23)–(3.28). On equating the $O(\epsilon)$ terms, (3.23) and (3.24) provide

$$2\left(1 + \frac{3}{4}m\right)\mu_0 H_0\frac{\partial}{\partial r}\left[\frac{\partial u_1}{\partial r} + \frac{u_1}{r}\right] + 3E\mu_0\frac{\partial H_1}{\partial r} = \frac{1}{2}H_0\frac{\partial H_1}{\partial r}, \tag{3.34}$$

$$\frac{\partial H_1}{\partial t} + \frac{1}{r}\frac{\partial}{\partial r}\left[r(H_0u_1 + u_0H_1)\right] = 0, \tag{3.35}$$

where we have used the first-order correction to the viscosity (3.25), namely

$$\mu_1 = \frac{m\mu_0}{2E}\left(\frac{\partial u_1}{\partial r} + \frac{u_1}{r}\right). \tag{3.36}$$

Boundary conditions (3.26) and (3.27) give

$$u_1 = 0 \qquad (r = 0), \tag{3.37}$$

$$\left(1 + \frac{3}{4}m\right)\mu_0\left(\frac{\partial u_1}{\partial r} + \frac{u_1}{r}\right) = \frac{1}{8}H_1 + \frac{\mu_0 u_1}{2r} \quad (r = R_0), \tag{3.38}$$

and the frontal-evolution and volume-conservation equations (3.28*a*,*b*) give

$$\dot{R}_1 = u_1(R_0, t) + ER_1, \quad \int_0^{R_0} rH_1\,\mathrm{d}r = -H_0R_0R_1. \tag{3.39a,b}$$

Equation (3.34) can be integrated and simplified using (3.29) to give

$$\left(1 + \frac{3}{4}m\right)\mu_0\left(\frac{\partial u_1}{\partial r} + \frac{u_1}{r}\right) = \frac{1}{8}H_1 + A(t), \tag{3.40}$$

where A is the constant of integration. On evaluating this equation at $r = R_0$, and comparing with condition (3.38), we deduce that

$$A(t) = \frac{\mu_0}{2R_0}u_1(R_0, t). \tag{3.41}$$

It is possible to derive a second expression relating A and $u_1(R_0, t)$ by first rewriting (3.40) in the form

$$\left(1 + \frac{3}{4}m\right)\mu_0\frac{\partial}{\partial r}(ru_1) = \frac{1}{8}rH_1 + A(t)r, \tag{3.42}$$

and then integrating from $r = 0$ to $r = R_0$ to give

$$\left(1 + \frac{3}{4}m\right)\mu_0\left[ru_1\right]_0^{R_0} = \frac{1}{8}\int_0^{R_0} rH_1\,\mathrm{d}r + \frac{1}{2}A(t)R_0^2. \tag{3.43}$$

The integral in this equation can be evaluated using (3.39*b*) to give

$$\left(1 + \frac{3}{4}m\right)\mu_0 u_1(R_0, t) = -\frac{1}{8}H_0R_1 + \frac{1}{2}A(t)R_0. \tag{3.44}$$

Substituting (3.41) into (3.44), and making u_1 the subject, we obtain

$$u_1(R_0, t) = \frac{-H_0R_1}{6(1 + m)\mu_0} = -2nER_1. \tag{3.45}$$

Substituting (3.45) into the frontal evolution equation (3.39*a*), we obtain

$$\dot{R}_1 = \frac{(1 - 2n)}{2n}t^{-1}R_1 \quad \text{and hence} \quad R_1(t) = R_1(1)t^{(1-2n)/2n} \tag{3.46a,b}$$

on integration. Equation (3.46*b*) shows that radial perturbations to the frontal position R_1 evolve independently of the thickness perturbation. This is remarkable given that, as we have noted, integration of (2.1) for the velocity $\boldsymbol{u}$ typically depends globally on the thickness H. However, in this case, the viscous force on the left-hand side of (3.42) is an exact differential, while the integral of buoyancy forces on the right-hand side

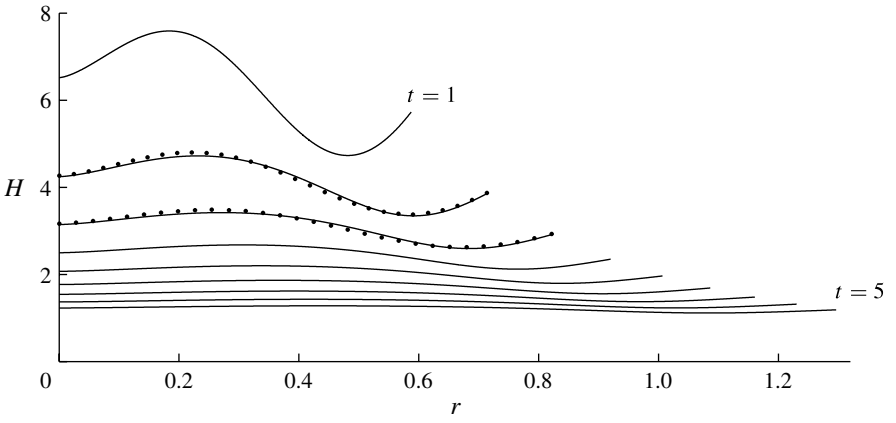

FIGURE 2. Numerical solution of the full nonlinear equations (3.11)–(3.15) for the evolution of the thickness H in the Newtonian case ($n = 1$) of an axisymmetric finite-volume release, plotted at progressive non-dimensional time intervals of 0.5, from a sample initial condition imposed at $t = 1$, up to $t = 5$ (solid). We plot as dotted curves the asymptotic prediction (3.50) at $t = 1.5$ and $t = 2$, which are seen to agree closely with the numerical solution. The convergence of the solution towards the uniform asymptotic state (3.29) is also illustrated.

has a value that is given by the volume-conservation equation (3.39*b*). Comparison of (3.46*b*) with (3.29) shows that the relative magnitude of the perturbation to the frontal position decays as $R_1/R_0 \propto t^{-1}$ at large times. Notably, the rate of relative decay is independent of n, which reflects the fact that R_1 simply corresponds to a time–displacement perturbation of the asymptotic similarity solution (3.29) (cf. Leppinen & Lister 2003).

Combining (3.45) and (3.41), we determine that

$$A(t) = -\frac{nH_0}{12R_0}R_1. \tag{3.47}$$

Substituting the left-hand side of (3.42) into (3.35), we obtain the evolution equation

$$\frac{\partial H_1}{\partial t} + \frac{E}{r}\frac{\partial}{\partial r}(r^2 H_1) + \frac{12E}{1+\frac{3}{4}m}\left(\frac{1}{8}H_1 + A\right) = 0. \tag{3.48}$$

We solve this equation analytically by first recasting it in terms of the similarity variable $\eta \equiv t^{-1/2n}r$ to give

$$t\frac{\partial H_1}{\partial t} + qH_1 = \frac{2n}{n+3}\frac{H_0 R_1}{R_0}, \tag{3.49}$$

where $q \equiv (4n+3)/[n(n+3)]$ and the partial derivative $\partial H_1/\partial t$ is understood to be taken with η fixed. Integration of (3.49) gives finally

$$H_1 = h_1(t^{-1/2n}r)t^{-q} - \frac{2H_0R_1}{R_0}\left(1 - t^{n/(n+3)}\right), \tag{3.50}$$

where $h_1(r) \equiv H_1(r, 1)$ denotes the initial perturbation to the thickness. The first term in the solution (3.50) shows that the perturbation to the similarity solution (3.29) retains its initial shape h_1 but decays as t^{-q}. This decay is illustrated in the Newtonian case $n = 1$ in figure 2, where we have plotted a numerical solution of the full

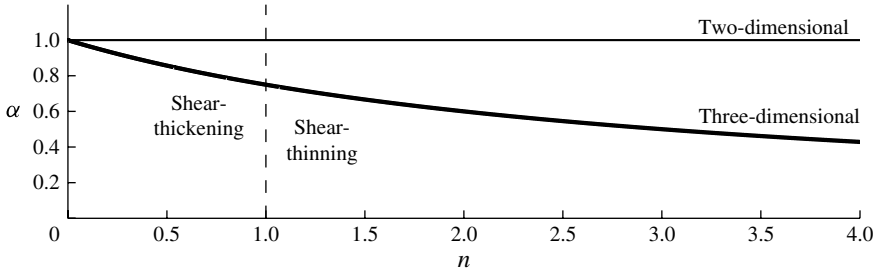

FIGURE 3. Large-time rate of relative decay α, as defined by $H_1/H_0 \propto t^{-\alpha}$, for the two-dimensional (thin) and three-dimensional (bold) releases plotted against the exponent n of the power-law rheology. Notably, α is independent of n in the two-dimensional case but decreases with n in the three-dimensional case, as implied by (3.10) and (3.51), respectively.

(nonlinear) equations (3.23)–(3.28) for an example perturbation. The second term in (3.50) describes a uniform perturbation of the thickness that is equivalent to a small change in time origin of the asymptotic state (3.29).

The perturbation (3.50) decays relative to the leading-order similarity solution according to

$$H_1/H_0 \propto t^{-3/(n+3)} \equiv t^{-\alpha} \quad (t \gg 1) \tag{3.51}$$

at large times. Notably, the rate of relative decay $\alpha \equiv 3/(n+3)$ in (3.51) decreases with n, so shear-thinning leads to a slower rate of relative decay. This dependence on n, which is illustrated in figure 3, can be contrasted with the rate of relative decay of a perturbation in the two-dimensional case (3.10), which was given by $\alpha = 1$ for all n.

4. Influence of surface tension

In this section, we consider the influence of a constraining surface tension on the evolution of the finite-volume release by allowing $\gamma > 0$ in the dynamic boundary condition (2.4). We begin by noting that the buoyancy and capillary forces on the right-hand side of (2.4) are comparable if the thickness at the edge is comparable to

$$\mathscr{H}_c \equiv \sqrt{2\gamma/\rho g'}. \tag{4.1}$$

Moreover, an exact balance between these forces can be achieved with

$$H = \mathscr{H}_c \quad \text{and} \quad \boldsymbol{u} = \boldsymbol{0}, \tag{4.2}$$

which is a static solution of the general equations (2.1)–(2.4). Some experimental confirmation of the static solution (4.2) has been provided by Sebilleau *et al.* (2010).

The governing equations for an axisymmetric finite-volume release subject to surface tension are the same as those presented in § 3.2, except we replace the dynamic condition (3.15) with the generalized form

$$2\mu\left[2\frac{\partial u}{\partial r} + \frac{u}{r}\right] = \frac{1}{2}\rho g' H - \gamma H^{-1} \quad (r = R), \tag{4.3}$$

which is the axisymmetric form of (2.4). Using (4.1), we define the scales

$$\mathscr{M}_c \equiv \left[\tilde{\mu}\,(\rho g'\mathscr{H}_c)^m\right]^n, \quad \mathscr{L}_c \equiv \left(\frac{V}{2\pi\mathscr{H}_c}\right)^{1/2}, \quad \mathscr{T}_c \equiv \frac{\mathscr{M}_c}{\rho g'\mathscr{H}_c}, \tag{4.4}$$

which characterize the viscosity, radius and time on which buoyancy drives a layer with thickness (4.1). We use (4.1) and (4.4) to non-dimensionalize the system according to

$$r \equiv \mathscr{L}_c \hat{r}, \quad t \equiv \mathscr{T}_c \hat{t}, \quad H \equiv \mathscr{H}_c \hat{H}, \quad u \equiv (\mathscr{L}_c/\mathscr{T}_c)\hat{u}, \quad \mu \equiv \mathscr{M}_c \hat{\mu}. \tag{4.5}$$

On dropping hats, the non-dimensional system is equivalent to (3.23)–(3.28), except we replace (3.27) with

$$\mu\left[2\frac{\partial u}{\partial r} + \frac{u}{r}\right] = \frac{1}{4}\left(H - H^{-1}\right) \quad (r = R). \tag{4.6}$$

As in § 3.2, we impose a point release (3.18), or equivalently

$$H \to \infty \quad (t \to 0). \tag{4.7}$$

We find solutions to the system given by (3.23)–(3.26), (3.28), (4.6) and (4.7) by trying an ansatz in which we take the thickness to be uniform at all times, so $H = H(t)$ only. With this simplification, (3.23) with (3.25) can be integrated subject to (3.26) to provide the velocity and viscosity

$$u = Er, \quad \mu = |E|^m, \tag{4.8a,b}$$

respectively, where $E(t)$ is a uniform rate of extension. Substitution of (4.8*a,b*) into (3.24) and (4.6) determines the equations

$$\frac{\mathrm{d}H}{\mathrm{d}t} + 2EH = 0, \quad 3E|E|^m = \frac{1}{4}(H - H^{-1}), \tag{4.9a,b}$$

respectively. Using (4.9*b*) to eliminate E in (4.9*a*), we obtain the evolution equation

$$\frac{\mathrm{d}H}{\mathrm{d}t} = -2\varsigma H\left|\frac{1}{12}\left(H - H^{-1}\right)\right|^n, \tag{4.10}$$

where $\varsigma \equiv \mathrm{sgn}(H-1)$.

For the Newtonian case, $n = 1$, we can integrate (4.10) analytically subject to (4.7) to give

$$H = \coth(t/6) \quad (n = 1), \tag{4.11}$$

which we have shown as a bold curve in figure 4. Given the initial condition of a point release (4.7), the second term on the right-hand side of (4.10), which represents surface tension, is negligible for $t \ll 1$; the gravity-driven similarity solutions (3.29) therefore describe the leading-order flow at early times. To determine the solutions in non-Newtonian cases $n \neq 1$, we solve (4.10) numerically using a Runge–Kutta scheme, which we initialize using the similarity solutions (3.29). Our solutions in the shear-thickening case $n = 1/2$ and the shear-thinning case $n = 3$ are plotted as thin curves in figure 4.

The early-time similarity solutions (3.29) imply that the layer initially undergoes significant gravity-driven extension with $E \gg 1$ at early times. Therefore, shear-thinning cases thin faster than shear-thickening cases at early times. At large times, the layer converges towards the equilibrium state (4.2) with a rate of approach that depends strongly on the power-law exponent n. In particular, while the shear-thinning and Newtonian cases $n \geqslant 1$ are seen to approach the equilibrium thickness $H = 1$ as $t \to \infty$, the shear-thickening case attains it in finite time T.

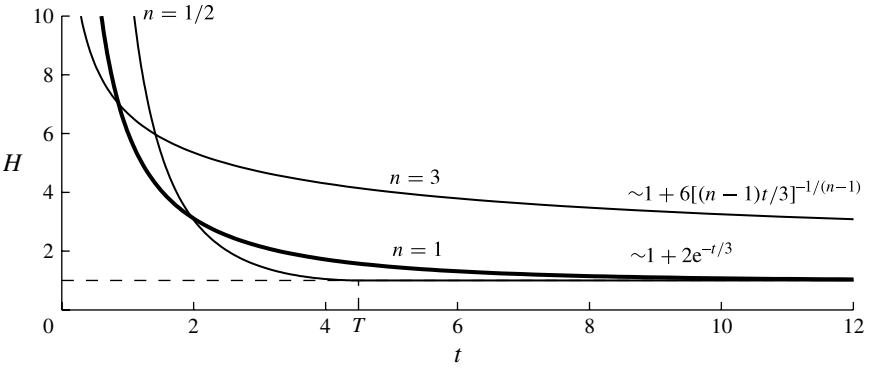

FIGURE 4. Evolution of the thickness of a finite-volume release subject to a constraining surface tension for $n = 1/2$ (shear-thickening), $n = 1$ (Newtonian) and $n = 3$ (shear-thinning). The Newtonian case is shown as a bold curve. The asymptote $H = 1$, towards which the thickness converges in all cases of n, is shown as a dashed line. As given by (4.14), the approach towards $H = 1$ occurs algebraically and exponentially over an infinite time in the shear-thinning and Newtonian cases, respectively, but is attained in a finite time $T \approx 4.5$ in the shear-thickening case. The algebraic decay in the shear-thinning case $n = 3$ is notably slow.

In order to understand the asymptotic approach of the solutions towards $H = 1$, we consider the evolution of a small perturbation from it, namely

$$H(t) = 1 + \tilde{H}(t), \tag{4.12}$$

where $\tilde{H} \ll 1$. Substitution of (4.12) into (4.10) determines the leading-order equation

$$\frac{\mathrm{d}\tilde{H}}{\mathrm{d}t} \sim -2\left(\frac{1}{6}\tilde{H}\right)^n \quad (H \to 1), \tag{4.13}$$

where we have specialized to the case in which the layer thins towards the equilibrium, so $\tilde{H} > 0$ and $\varsigma = 1$. By considering the solutions of (4.13), we can deduce that the asymptotic behaviour of the thickness as $H \to 1$ is described by

$$H \sim \begin{cases} 1 + 6\,[(n-1)t/3]^{-1/(n-1)} & (n > 1, t \to \infty), \\ 1 + 2\mathrm{e}^{-t/3} & (n = 1, t \to \infty), \\ 1 + 6\,[(1-n)(T-t)/3]^{1/(1-n)} & (n < 1, t \to T), \end{cases} \tag{4.14a,b,c}$$

where T is a constant of integration. The approach towards $H = 1$ is thus algebraic in non-Newtonian cases $n \neq 1$, but exponential in the Newtonian case $n = 1$. Notably, (4.14*a,b*) describe a large-time approach towards $H = 1$, while (4.14*c*) describes a finite-time approach ($t \to T$). In the shear-thickening case (4.14*c*), we note that (4.14*c*) applies only if $t \leqslant T$; otherwise, the term inside the square brackets is negative. However, (4.10) implies that the layer subsequently remains static, so $H = 1$ for $t > T$.

The rates of decay described by (4.14) are extremely sensitive to n. For example, the Newtonian case $n = 1$ decreases to within 10 % of the equilibrium thickness after $t \approx 10$, but the shear-thinning case $n = 3$ does this after the significantly greater time $t \approx 6000$. This dramatic contrast can be attributed to the fact that, as the layer approaches the static state (4.8*b*), the viscosity (4.8*b*) tends to infinity in shear-thinning cases $m < 0$, but tends to zero in shear-thickening cases $m > 0$.

Notably, the rates of attraction towards the asymptotic state (4.14) are significantly more sensitive to n compared with those of perturbations from the uniformly stretching asymptotic similarity solutions (3.51) considered in § 3.2. This contrast can be explained by noting that the former describes a perturbation to a static equilibrium, and is thus sensitive to the zero-strain singularity of the power-law rheology, whereas the latter describes a perturbation to a continuously flowing state.

Solutions of (4.10) subject to initial conditions in which $H(0) < 1$ also describe the thickening of an overextended layer as it relaxes back to equilibrium under the influence of surface tension. The asymptotes (4.14*a,b,c*) also apply in these cases, but with negative signs replacing the positive signs in front of the second terms.

Our analysis has shown that the equilibrium thickness (4.1) provides a threshold below which the current does not thin. The potential for this threshold to significantly influence the dynamics of a spreading viscous layer forms an important consideration in the experimental study of Pegler & Worster (2012).

5. Conclusions

We have shown that a thin layer of viscous power-law fluid released over an inviscid fluid evolves with qualitatively distinct behaviours in the two cases of the coefficient of total surface tension $\gamma = 0$ and $\gamma > 0$. In the case $\gamma = 0$, both the two-dimensional and axisymmetric releases converge towards similarity solutions with uniform thickness profiles. The frontal position of these similarity solutions evolves as $t^{1/n}$ and $t^{1/2n}$ in the two- and three-dimensional releases, respectively, where n is the power-law exponent.

In the two-dimensional case, perturbations from the similarity solution decay relative to the similarity solution as t^{-1}. Notably, this rate of relative decay is independent of n. In the three-dimensional case, any small axisymmetric perturbation from the similarity solution evolves as a superposition of a scaled initial shape and a uniform perturbation that is equivalent to a small change in time origin of the asymptotic state. The large-time rate of relative decay of the perturbation $t^{-3/(n+3)}$ decreases with the power-law exponent n. For example, it is $t^{-3/4}$ for Newtonian fluid with $n = 1$, and $t^{-1/2}$ for the shear-thinning case $n = 3$, which is relevant to the case of glacial ice modelled using Glen's flow law.

In the case of a constraining surface tension $\gamma > 0$ our solutions of the generalized model equations show that the layer converges towards a static state of uniform thickness $\sqrt{2\gamma/\rho g'}$. The asymptotic form of this convergence was shown to depend strongly on n, with rapid finite-time algebraic decay in shear-thickening cases, large-time exponential decay in the Newtonian case and slow large-time algebraic decay in shear-thinning cases.

The results of this paper in the case $\gamma = 0$ may indicate some general properties of relevance to glacial ice dynamics, such as the potential for markedly slow attraction of ice shelves towards asymptotic states.

REFERENCES

DiPietro, N. D. & Cox, R. G. 1979 The spreading of a very viscous liquid on a quiescent water surface. *Q. J. Mech. Appl. Maths* **32**, 355–381.

Dorsey, C. W. & Manga, M. 1998 The low-Reynolds number spreading of axisymmetric drops and gravity currents along a free surface. *Phys. Fluids* **10**, 3011–3013.

Foda, M. & Cox, R. G. 1980 The spreading of liquid films on a water–air interface. *J. Fluid Mech.* **101**, 33–51.

HOULT, D. P. 1972 Oil spreading on the sea. *Annu. Rev. Fluid Mech.* **4**, 341–368.

HOWELL, P. D. 1994 Extensional thin layer flows. PhD thesis, University of Oxford.

KOCH, D. M. & KOCH, D. L. 1995 Numerical and theoretical solutions for a drop spreading below a free fluid surface. *J. Fluid Mech.* **287**, 251–278.

LEPPINEN, D. & LISTER, J. R. 2003 Capillary pinch-off in inviscid fluids. *Phys. Fluids* **15** (2), 568–578.

LISTER, J. R. & KERR, R. C. 1989 The propagation of two-dimensional and axisymmetric viscous gravity currents at a fluid interface. *J. Fluid Mech.* **203**, 215–249.

PATERSON, W. S. B. 1994 *The Physics of Glaciers*, 3rd edn. Pergamon.

PEGLER, S. S. & WORSTER, M. G. 2012 Dynamics of a viscous layer flowing radially over an inviscid ocean. *J. Fluid Mech.* **696**, 152–174.

ROBISON, R. A. V., HUPPERT, H. E. & WORSTER, M. G. 2010 Dynamics of viscous grounding lines. *J. Fluid Mech.* **648**, 363–380.

SEBILLEAU, J., LEBON, L., LIMAT, L., QUARTIER, L. & RECEVEUR, M. 2010 The dynamics and shapes of a viscous sheet spreading on a moving liquid bath. *Europhys. Lett.* **92**, 14003.